# Supplementary Information

## Design Strategies for Ceria Nanomorphologies: Untangling Key Mechanistic Concepts

Yuwen Xu,[a,b] Sajjad S. Mofarah,[a] Rashid Mehmood,[a] Claudio Cazorla,[a] Pramod Koshy[a], and Charles C. Sorrell[a,c]

School of Materials Science and Engineering, UNSW Sydney, Sydney, NSW 2052, Australia

[a] School of Materials Science and Engineering, UNSW Sydney, Australia
[b] E-Mail: yuwena17@163.com
[c] C.Sorrell@unsw.edu.au

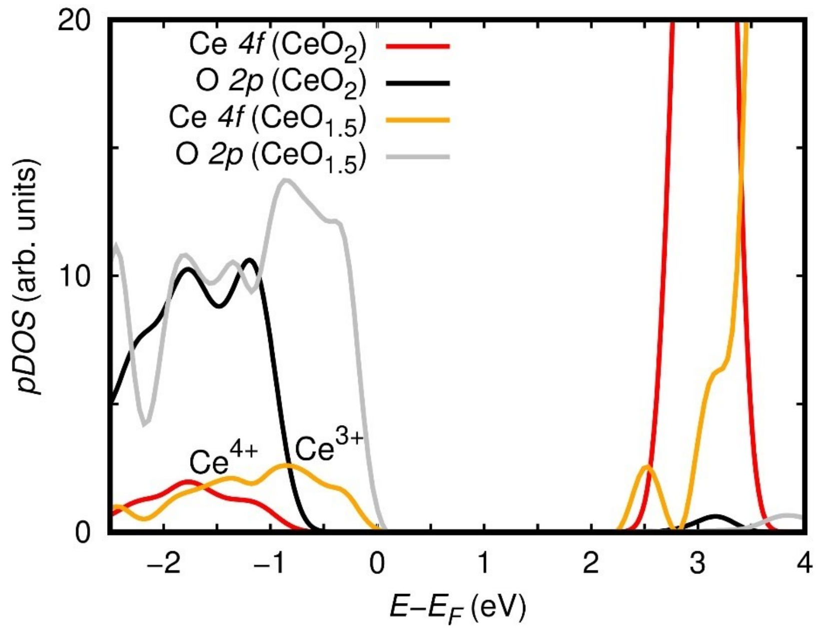


Figure S1. Partial density of electronic states estimated for bulk $CeO_2$ and $CeO_{1.5}$ using first-principles methods based on the hybrid DFT functional HSE06[a] (authors' unpublished work)

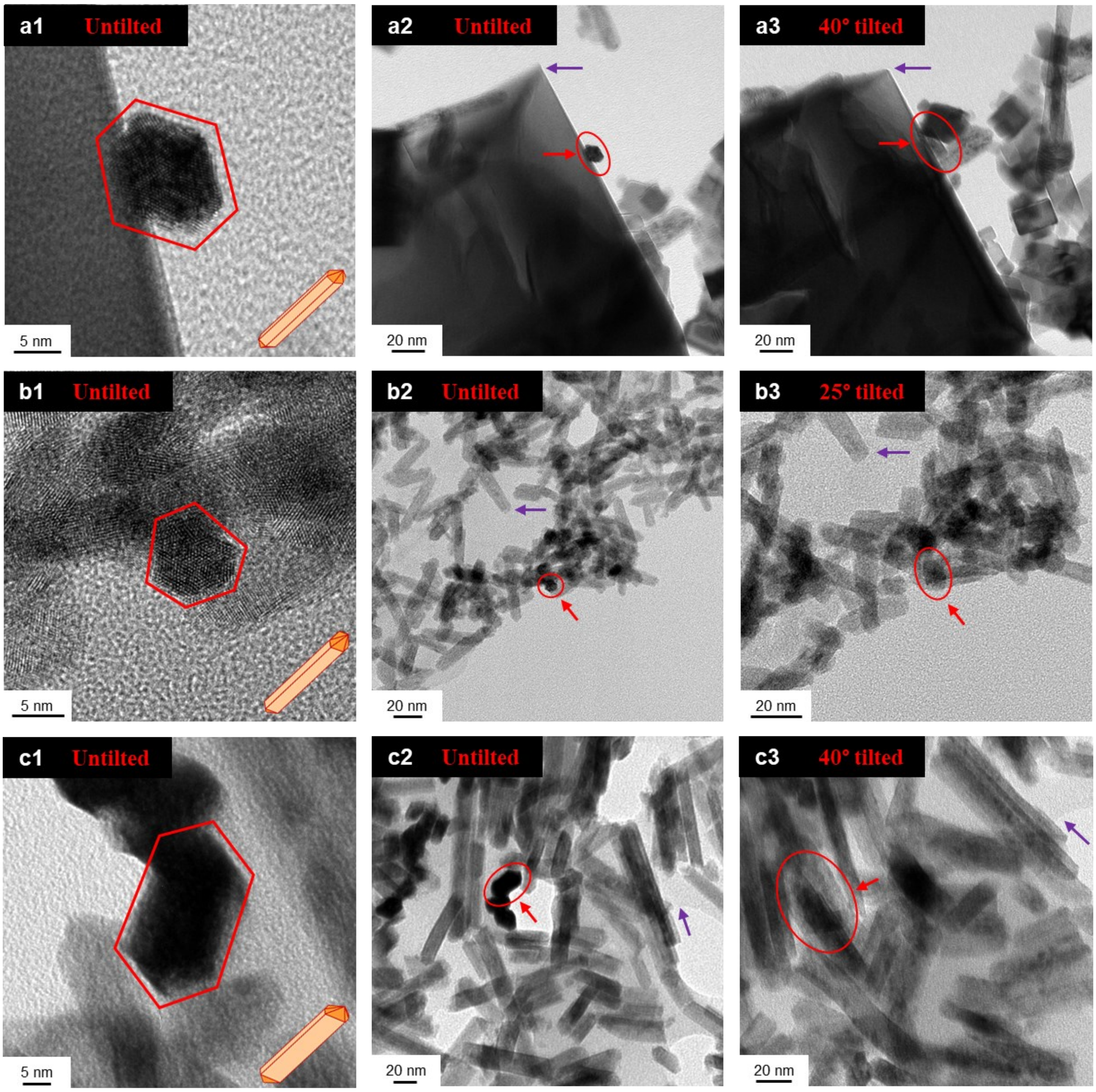


Figure S2. TEM images of the nanorods prepared at high [Ce] and high [NaOH]: (a1) high-magnification top view of nanorod, showing elongated hexagonal cross section; (a2) low-magnification untilted top view of nanorods on nanocube; (a3) low-magnification 40° tilted view of Figure (a2), confirming that the particle with hexagonal cross section is a nanorod; (b1) high-magnification top view of nanorod, showing asymmetric hexagonal cross section; (b2) low-magnification untilted top view of nanorods; (b3) low-magnification 25° tilted view of Figure (b2), confirming that the particle with hexagonal cross section is a nanorod; (c1) high-magnification top view of nanorods, showing compressed hexagonal cross section; (c2) low-magnification untiled top view of nanorods; (c3) low-magnification 40° tilted view of Figure (b2), confirming that the particle with hexagonal cross section is a nanorod (authors' unpublished work)

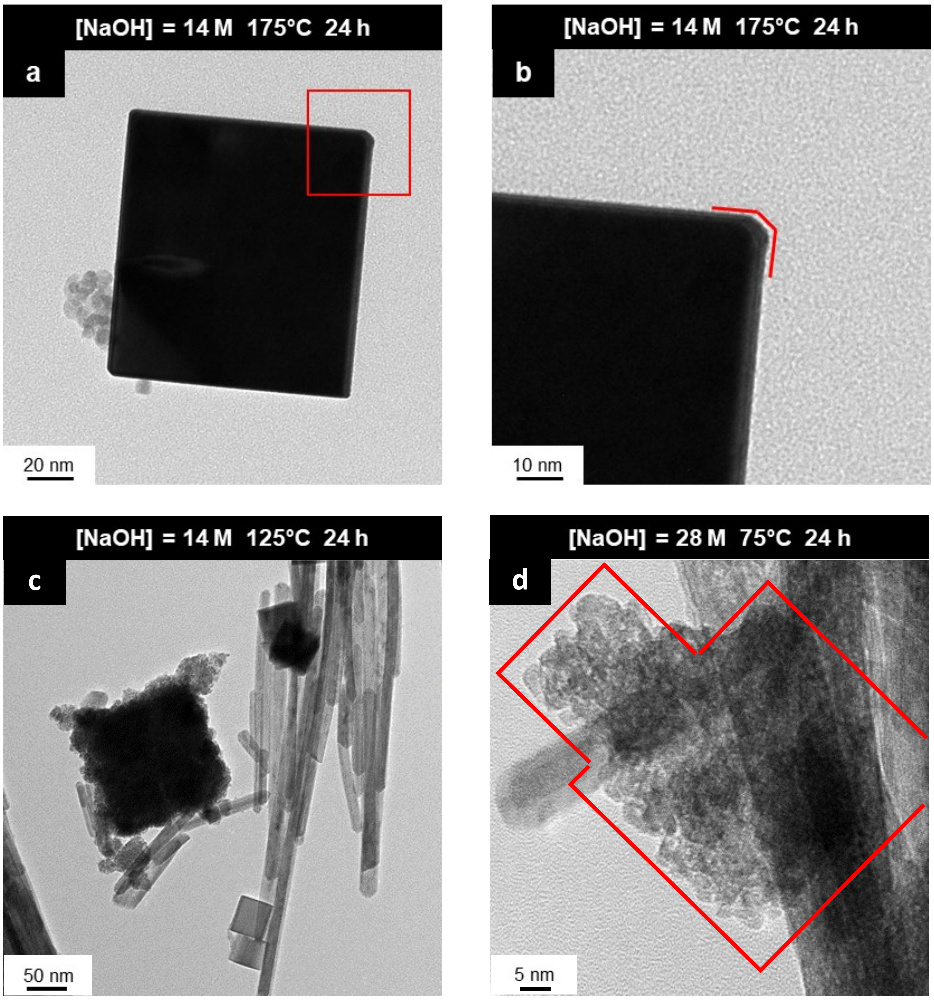


Figure S3. TEM images of: (a) {111} truncated nanocube; (b) enlargement of {111} truncation; (c) cuboid; (d) adjacent cuboids (authors' unpublished work)

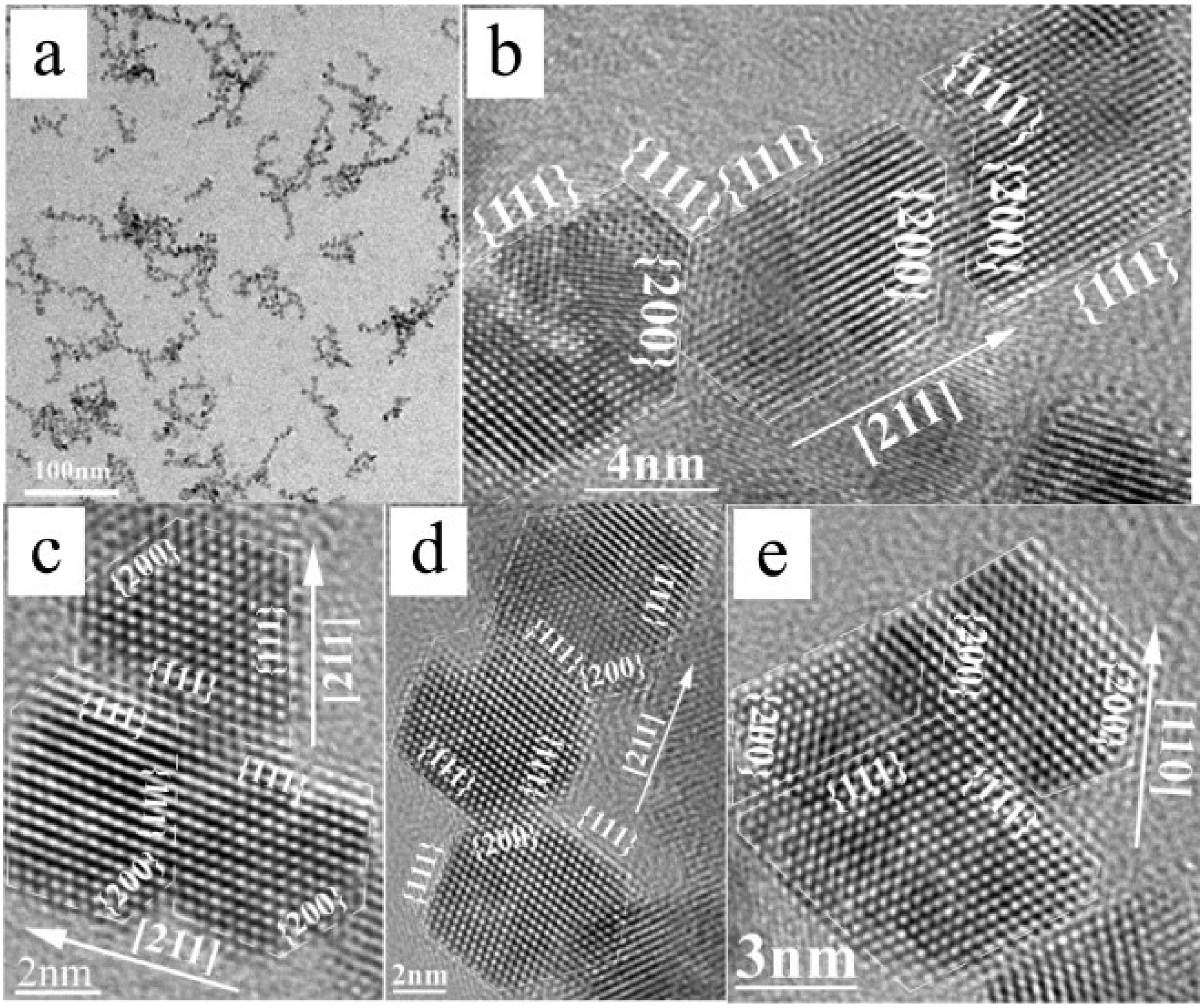


Figure S4. Oriented attachment of effectively {100} (but {200} as shown) truncated octahedra to form nanochains at 100°C,[b] reprinted with permission from American Chemical Society

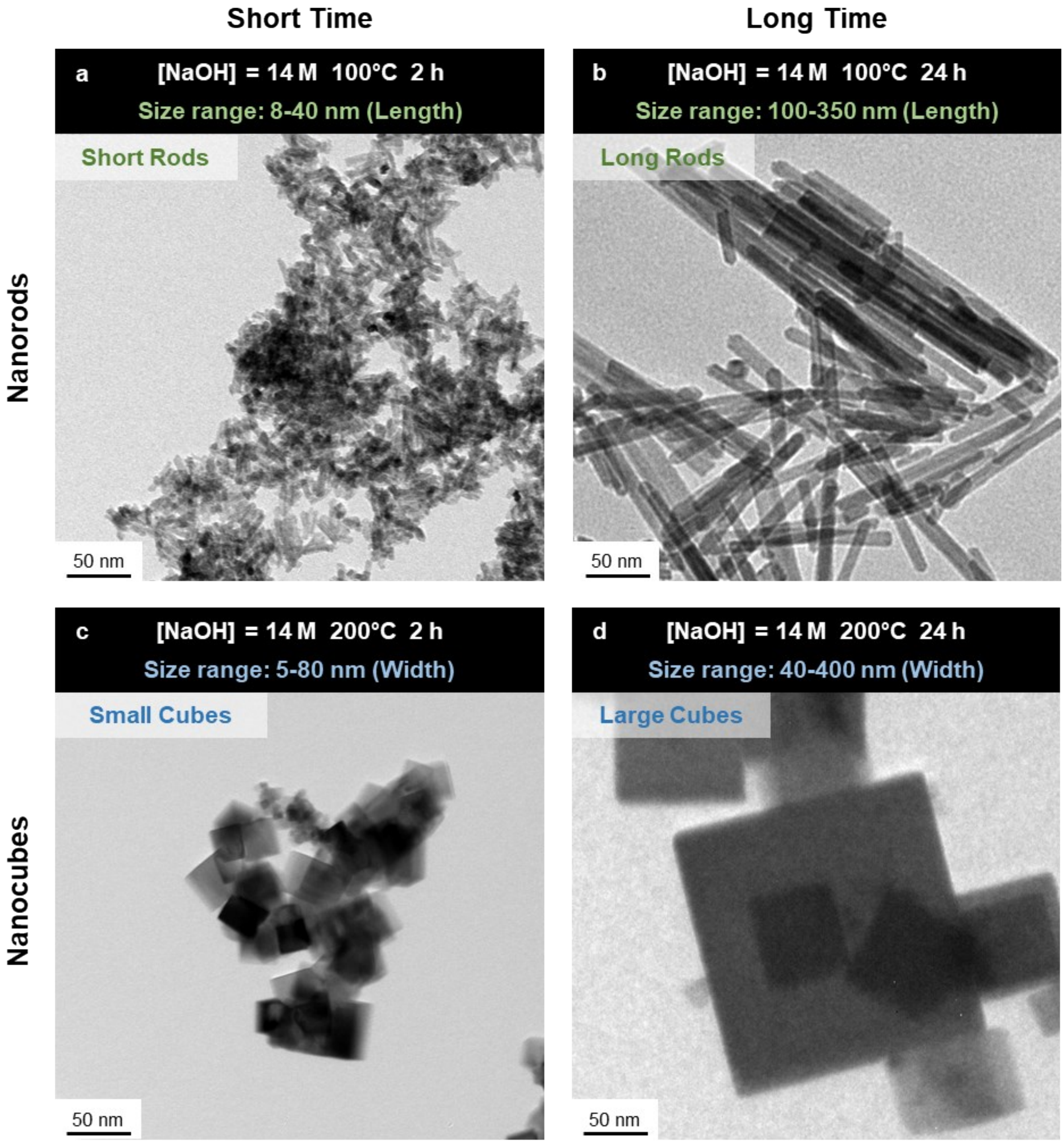


Figure S5. TEM images of: (a) short nanorods (short time); (b) long nanorods (long time); (c) small nanocubes (short time); (d) large nanocubes (long time) (authors' unpublished work)

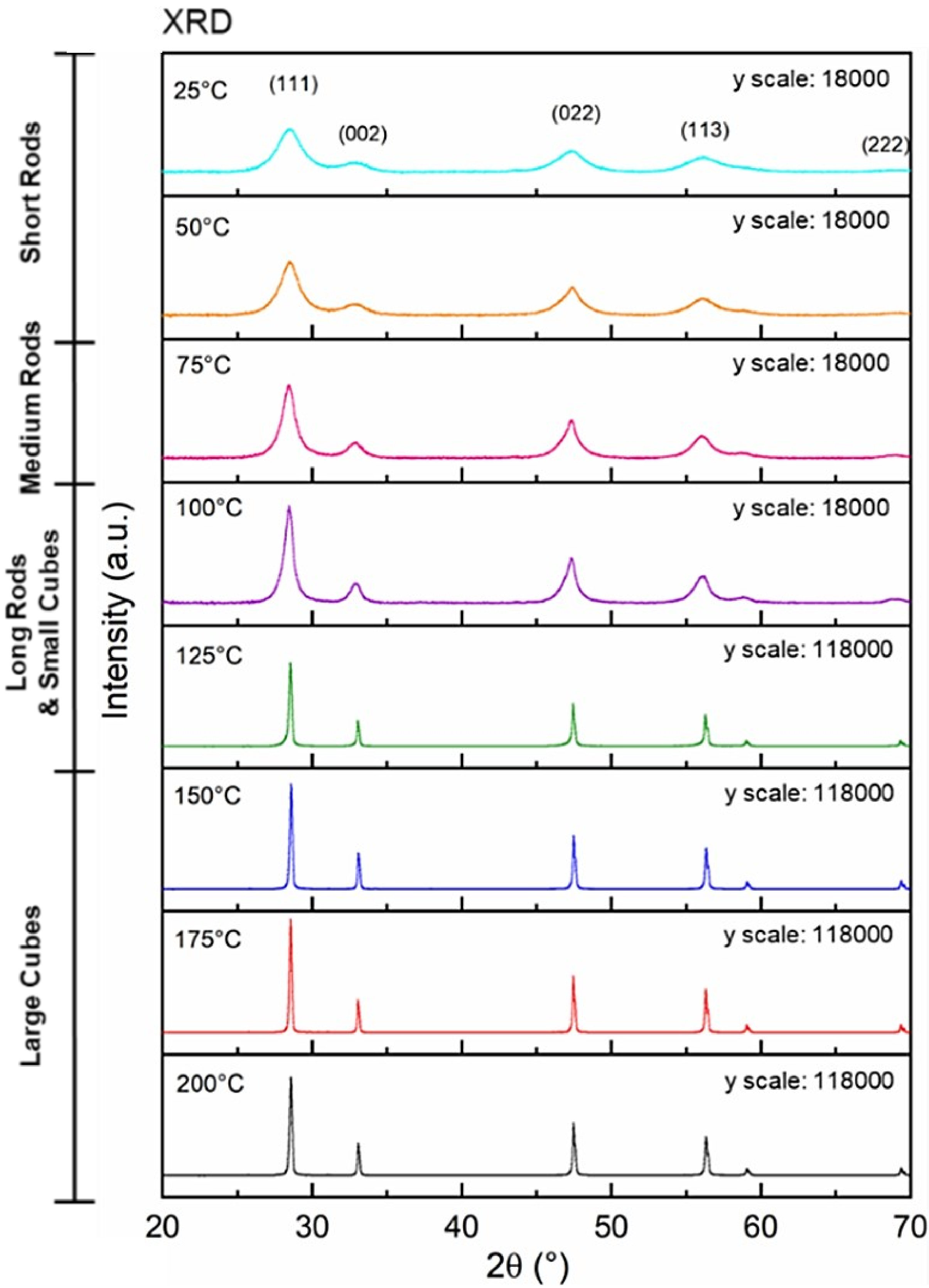


Figure S6. XRD spectra of $CeO_{2-x}$ synthesised at different temperatures (precipitated and hydrothermal); peak broadening with decreasing temperature indicates decreasing crystallite size as well as increasing amorphisation; shifts to higher 2θ angles indicate lattice expansion from ionic radii increase from $Ce^{4+} \rightarrow Ce^{3+}$ reduction, which occurs ownig to charge compensation for the introduction of oxygen vacancies ($V_O^{\bullet\bullet}$) (authors' unpublished work)

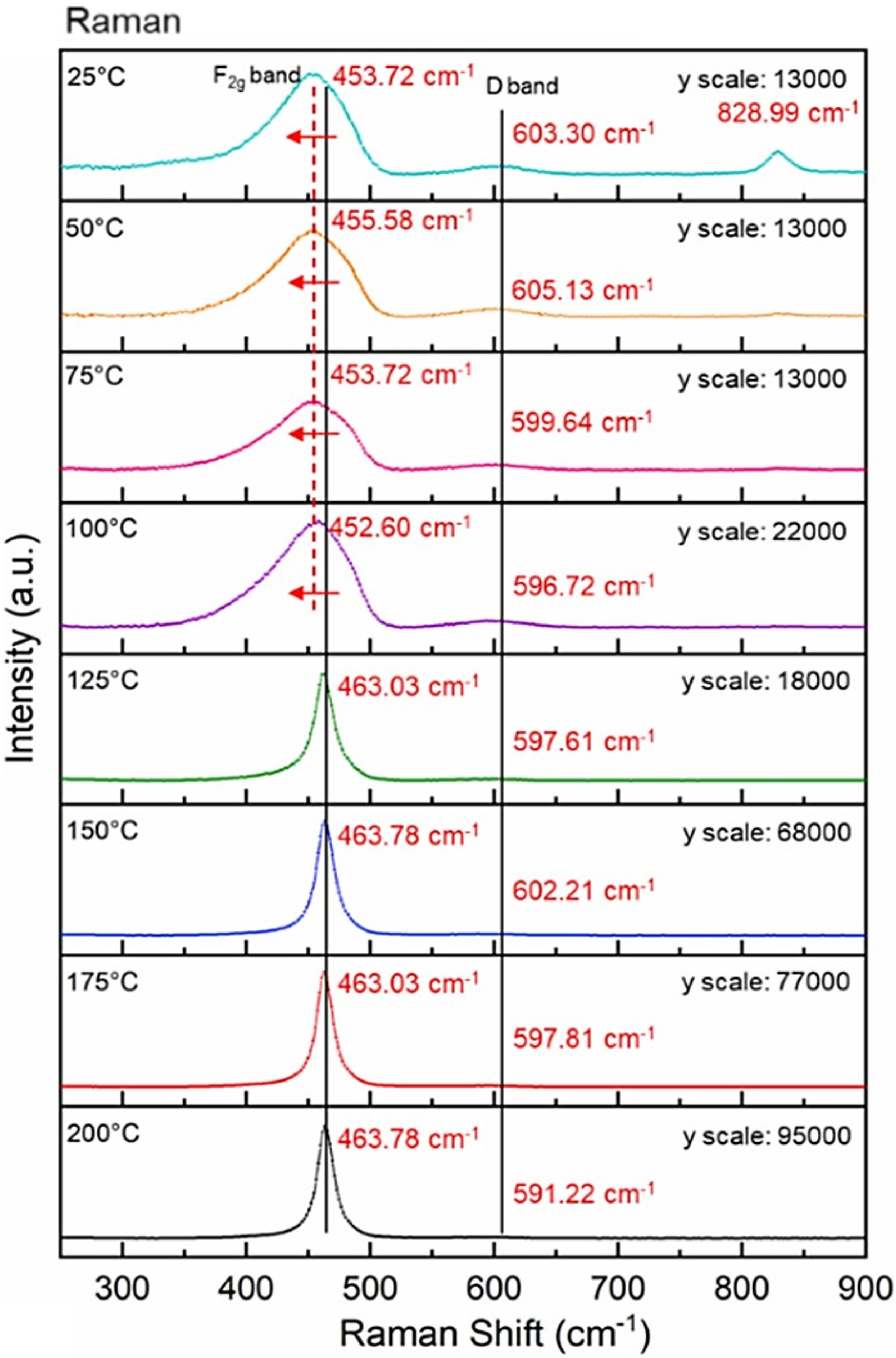


Figure S7. Laser Raman microspectra of $CeO_{2-x}$ obtained at different temperatures (precipitated and hydrothermal); blue shift of predominant peak at ~464 $cm^{-1}$ indicates increasing number of oxygen vacancies ($V_O^{\bullet\bullet}$); peak at ~600 $cm^{-1}$ confirms presence of oxygen vacancies ($V_O^{\bullet\bullet}$) (authors' unpublished work)

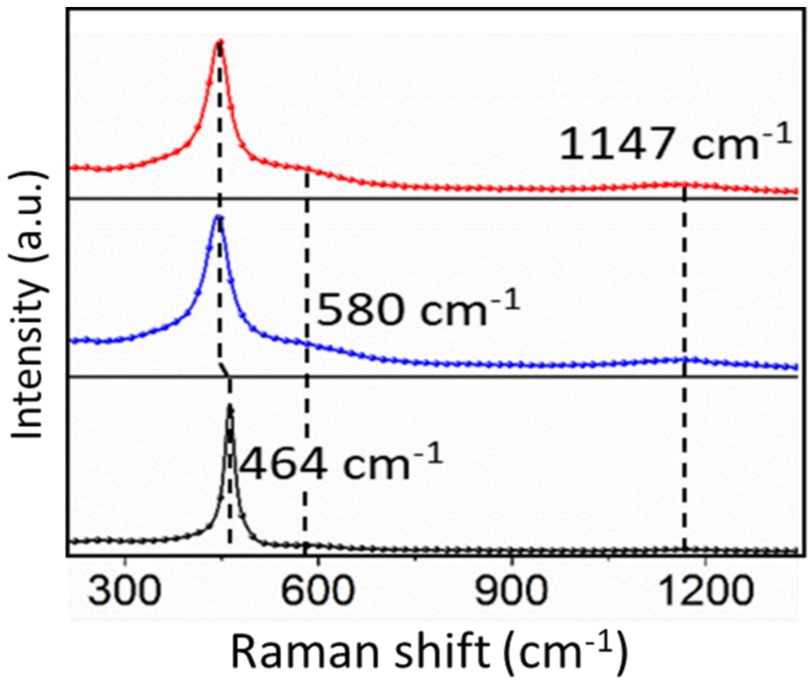


Figure S8. Laser Raman microspectra of $CeO_{2-x}$ with different oxygen vacancy concentrations; two peaks at ~580 cm$^{-1}$ and ~1147 cm$^{-1}$ indicate presence of oxygen vacancies (authors' unpublished work)

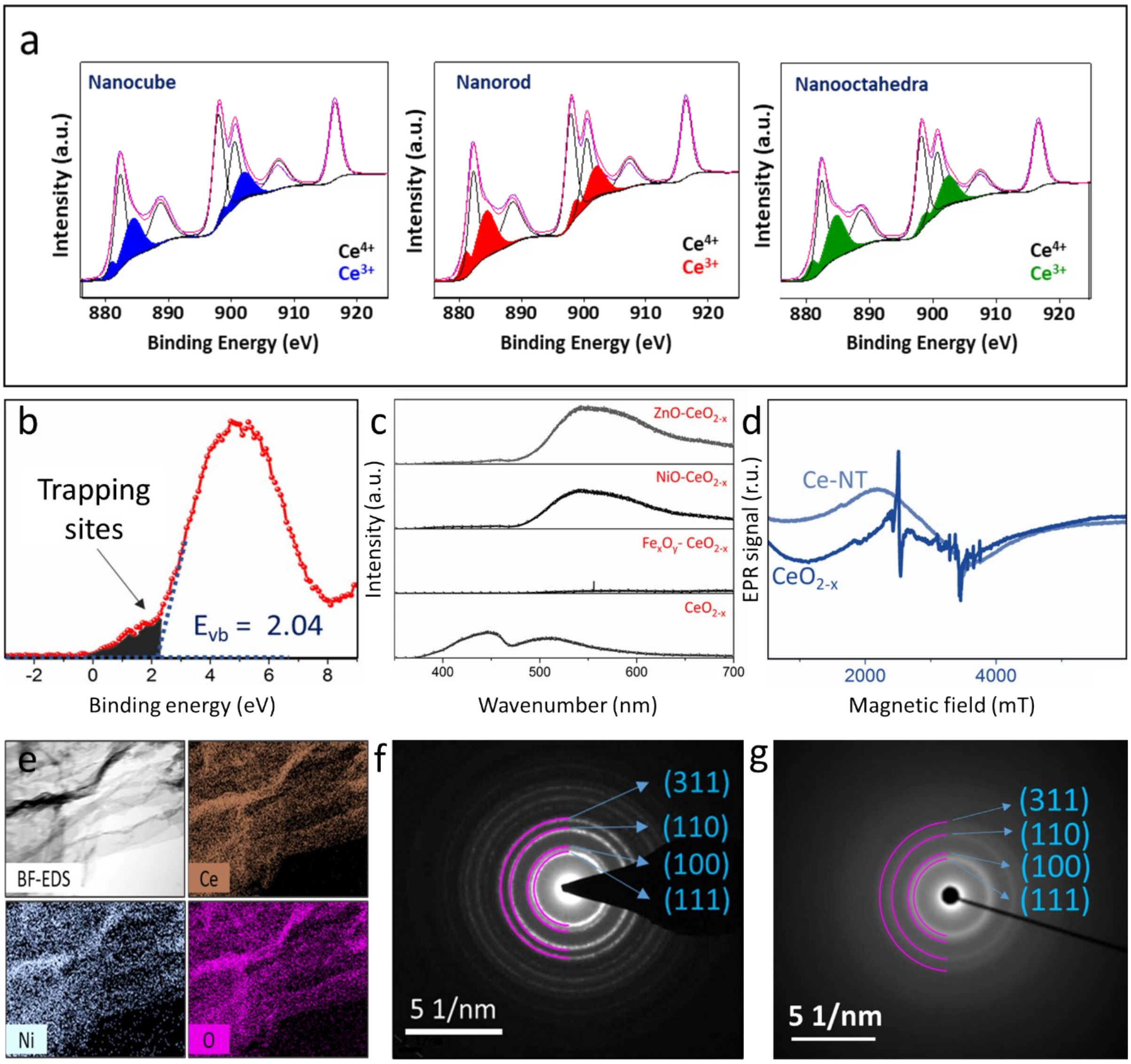


Figure S9. (a) XPS spectra of $CeO_{2-x}$ (shaded peaks for $Ce^{3+}$) for nanocubes, nanorods, and nanoctahedra; (b) XPS spectra of $CeO_{2-x}$, where role of defects in formation of trapping sites at binding energies ~2 eV is highlighted; (c) PL spectra of $CeO_{2-x}$ and $CeO_{2-x}$-based heterojunction nanostructures, where defects are responsible for intensity variations; (d) EPR spectra of $CeO_{2-x}$ and $CeO_2$ nanotube (NT); (e) TEM image and EDS mapping of $CeO_{2-x}$ nanosheets decorated with NiO nanoparticles; (f,g) SAED patterns of $CeO_{2-x}$ with low (f) and high (g) oxygen vacancy concentrations, as indicated by comparison of diffuse rings

(a) Adapted from authors' work[c])
(b) Adapted from authors' work[d]
(c) Adapted from authors' work[d]
(d) Authors' unpublished work
(e) Adapted from authors' work[d]
(f) Adapted from authors' work[d]
(g) Adapted from authors' work[d]

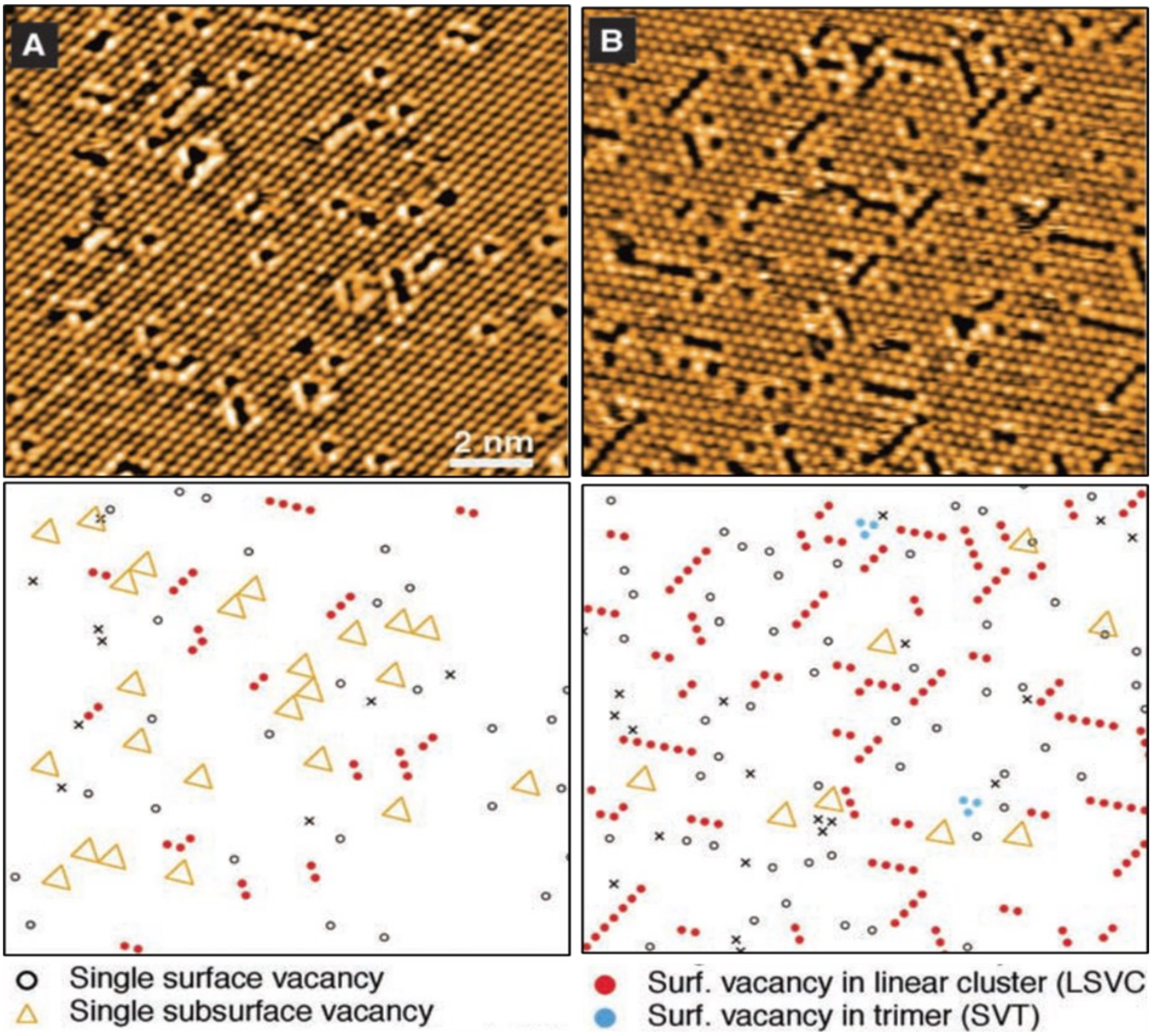

Figure S10. STEM images and reconstructions of (111) facet of $CeO_2$ after vacuum annealing for: (a) 1 min; (b) 5 min;[e] reprinted with permission from American Association for the Advancement of Science

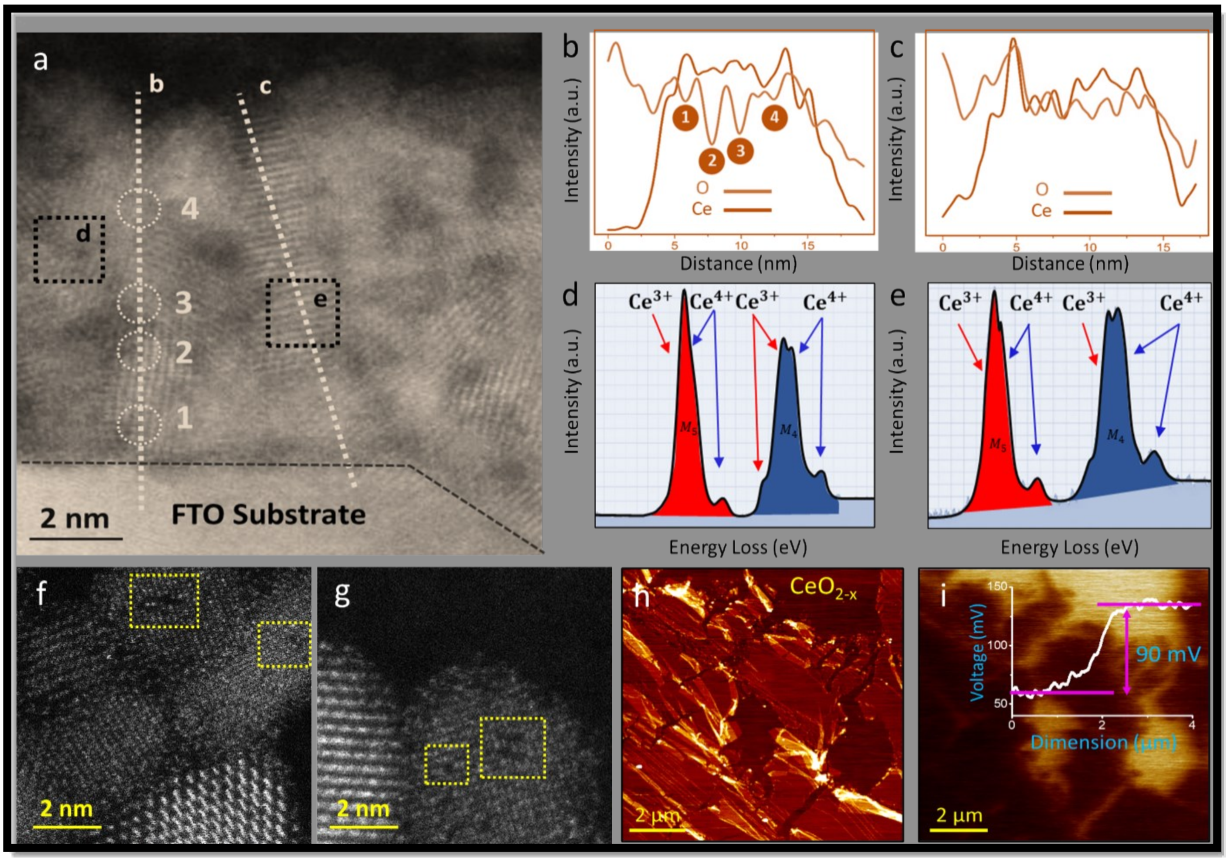


Figure S11. (a) HAADF image of nanostructure; (b) EDS line scan across crystallite boundaries; (c) EDS line scan within crystallite; (d) EELS spectra at crystallite boundary (black dotted box d in (a)); (e) EELS spectra within crystallite (black dotted box e in (a)); (f,g) HAADF images showing Ce vacancies within $CeO_{2-x}$ crystallites (highlighted by yellow boxes); (h,i) KPFM analysis of $CeO_{2-x}$ nanosheet (voltage profile in inset of (i)) (adapted from authors' work)

(a) Adapted from authors' work[f]
(b) Adapted from authors' work[f]
(c) Adapted from authors' work[f]
(d) Adapted from authors' work[d]
(e) Adapted from authors' work[d]
(f) Adapted from authors' work[d]
(g) Adapted from authors' work[d]
(h) Adapted from authors' work[d]
(i) Adapted from authors' work[d]

## References


[a] J. Heyd and G.E. Scuseria, *J. Chem. Phys.*, 2003, **118**, 8207-8215.

[b] N. Du, H. Zhang, B. Chen, X. Ma, and D. Yang, *J. Phys. Chem. C*, 2007, **111**, 12677-12680.

[c] R. Mehmood, N. Ariotti, J.L. Yang, P. Koshy, and C.C. Sorrell, *ACS Biomater. Sci. Eng.*, 2018, **4**, 1064-1072.

[d] S.S. Mofarah, E. Adabifiroozjaei, R. Pardehkhorram, M.H.N. Assadi, M. Hinterstein, Y. Yao, X. Liu, M.B. Ghasemian, K. Kalantar-Zadeh, R. Mehmood, C. Carzorla, R. Shahmiri, G. Bahmanrokh, S. Bhattacharyya, M.C. Spadaro, J. Arbiol, S. Lim, Y. Xu, H. Arandiyan, J. Scott, P. Koshy, and C.C. Sorrell, *Adv. Mater.*, 2019, **31**, Paper 1905288 {9 + 72 pp.}.

[e] F. Esch, S. Fabris, L. Zhou, T. Montini, C. Africh, P. Fornasiero, G. Comelli, and R. Rose, *Science*, 2005, **309**, 752-755.

[f] S.S. Mofarah, E. Adabifiroozjaei, Y. Yao, P. Koshy, S. Lim, R. Webster, X. Liu, R.K. Nekouei, C. Cazorla, Z. Liu, Y. Wang, N. Lambropoulos, and C.C. Sorrell, *Nature Comm.*, 2019, **10**, Paper 2594 {9 + 32 pp.}.